GENERATION OF ALTERNATIVE GEOLOGICAL MODELS FOR SPATIAL UNCERTAINTY IN A GEOTHERMAL CONTEXT

Ariel Vidal[1,2] and Rosalind Archer[1,2]

[1]Department of Engineering Science – The University of Auckland, New Zealand

[2]The Geothermal Institute, The University of Auckland, New Zealand

avid587@aucklanduni.ac.nz

Keywords: *Reservoir modelling, geological uncertainty, geostatistics, multiple point statistics*

ABSTRACT

Subsurface fluid flow modelling is highly dependent on the spatial distribution of geological units and rock properties. As can be expected this distribution is a priori unknown and only through direct sampling from well drilling or indirect geophysical methods this distribution can be constrained. However, the interpreted geological distribution needs to be treated as only one interpretation from a set of alternative scenarios.

In this paper we address the problem of geological uncertainty through the use of stochastic modelling and the use of multiple point statistics methods. An example from a real geothermal field is presented with a discussion and some conclusions.

1. INTRODUCTION

As in other similar problems related to subsurface fluid flow, rock properties and their spatial distribution are of primary interest. The modelling of these properties is not an easy task mainly for the lack of hard data but, as could be expected, spatially the rock properties follow some geological rules that make possible to model geological bodies that share some characteristics (same permeability for example) instead of treating each model cell as a separate unit. Normally, conceptual geological models of geothermal systems are built based on previous knowledge complemented with the available data and then these conceptual scenarios are used as a basis for numerical models. Unfortunately, no matter how much data we can collect from the field, it is practically impossible to get the full geological picture of the system without uncertainty, the conceptual model is just one representation of what the system could be. In this sense, geostatistical simulation has become a popular methodology for simulating unknown geological properties and geometries, and for quantifying reservoir heterogeneities. Geostatistics is a robust family of methodologies that allows to include available data into different realizations in a stochastic framework and that creates an easier link between simulations and geological knowledge.

Traditional geostatistical methods, such as kriging or sequential Gaussian simulation (Deutsch and Journel, 1998), require the estimation of an important indicator known as the variogram (Deutsch and Journel, 1998), which quantifies the correlation of a variable between two different locations. In a geothermal context there is a scarcity of data when compared, for example, with oil and gas or mining operations, which could make the calculation of the variogram unreliable. Additionally, traditional methods based on the inference of the variogram only measure the degree of correlation/connectivity between any two locations in space (two point statistics), so they cannot model geological structures such as channels, irregular geological units or complex fractures.

In this work we will focus on the use of a relatively new family of algorithms termed multiple point statistics models (MPS), which are a novel simulation approach based on the reproduction of spatial patterns present in a training image. In this methodology the geological structures are characterized by multipoint statistics, which expresses the joint variability at many more than two locations at the same time. Such multiple point statistics cannot be inferred from typically sparse well data but could be read from training images depicting the expected subsurface heterogeneities. In simple terms, a training image is a numerical representation of the geometry and distribution of objects/patterns deemed to prevail in the volume of interest (Journel, 1993). This training image allows us to avoid modelling the variogram explicitly and the conditional probabilities for sequential simulation are extracted from this training image. Ideally, these training images should reflect a prior conceptual geological scheme which includes any additional knowledge of the physical phenomena and the region of interest. For example, in a geothermal context, it is very likely that our region of interest may be located in a volcano-sedimentary setting where the periodic accumulation of volcanic products generates the local stratigraphy that should be expected in our conceptual model, so this volcanological prior knowledge may be used for the construction of a training image.

It is important to mention that, in the context of reservoir simulation and uncertainty quantification, geostatistical realizations are not an end-goal itself; instead these multiple realizations are normally used as inputs for flow simulators. One limitation with this approach is that each run of the numerical simulator may be very time consuming (on the order of several minutes to hours), which makes it unfeasible to evaluate each one of the realizations generated by the geostatistical algorithm (which could be on the order of hundreds or thousands of realizations for a characterization of the spatial uncertainty). Ideally, it is desirable to select only a small subset of these realizations for evaluation in the expensive flow simulator, but this subset should keep most of the variability present in the full ensemble of realizations. In this work a methodology to generate this reduced ensemble is introduced with an example with data from a real field and some insights about the use of this approach in conjunction with a calibration routine are presented.

2. GEOSTATISTICAL SIMULATION – MPS

Kriging, and its variants, works well for mining and other applications where local accuracy is of crucial importance. However, for subsurface flow problems kriging is not always appropriate as it produces a smooth image of variability which may have a large influence in flow behaviour. For a better reproduction of the spatial variation of a system stochastic simulation was introduced to deal with the smoothing effect of kriging and provide alternative realizations that displayed the spatial variation from a given variogram model (Matheron, 1973; Journel, 1974). The principle behind a geostatistical simulation consists of building a fictitious variable that reproduces the spatial continuity of the regionalized variable $z = \{z(x), x \in S\}$, where S represents a stationary field. This construction is based on the assumption that z is only one particular realization of a random function $Z = \{Z(x), x \in S\}$, so the basic idea is to generate a set of realizations of this random function to model subsurface heterogeneities and assess spatial uncertainties. One popular method to simulation is sequential Gaussian simulation (Goovaerts, 1997; Deutsch and Journel, 1998), which uses the properties of a Gaussian random function (a Gaussian random function is fully characterized by its mean and covariance). In the sequential Gaussian simulation algorithm the mean and variance of the Gaussian distribution at any location along the simulation path are estimated by the kriging estimate and the kriging variance, respectively. The value obtained from that distribution is then used as conditioning data to simulate the value of the random function at each location in the simulation grid.

In a similar way, MPS algorithms operate cell-wise with the conditional probabilities for each cell value being lifted as conditional proportions from a training image. In essence, the training image provides all the necessary multiple point covariance values. The decision of stationarity allows scanning a specific training image for replicates of the single multiple-point conditioning data event. By so doing one would sidestep any variogram/covariance modelling and also any kriging (Remy et al., 2009). Currently, there are several MPS algorithms being used in real applications which have shown reliable results such as SNESIM, FILTERSIM, DisPAT, IMPALA or Direct Sampling to name just a few (Strebelle, 2002; Wu et al., 2008; Honarkhah and Caers, 2010; Straubhaar et al., 2011; Mariethoz et al., 2010). It is beyond the scope of this paper to present a comparison between different algorithms or a detailed description for each of them, but instead to show some practical considerations for its use in the context of geothermal reservoir modelling. For a deeper and updated state of the art discussion about different MPS methods, readers are strongly advised to read the book: Multiple-point geostatistics, Stochastic modelling with training images (Mariethoz and Caers, 2015).

2.1 Training Images

As was previously mentioned, in kriging-based algorithms the variability of the random variable is implicitly done when choosing a variogram model. The equivalence with MPS algorithms is the selection of a training image. A training image is a repository of the patterns and their respective likelihoods for the problem under study. A frequent pattern appears more often in the training image than a rare one. An important point is that the actual position of a pattern in the training image is irrelevant, what matters is its presence and its frequency (Boucher, 2013). Figure 1 presents some examples of training images used for a variety of problems.

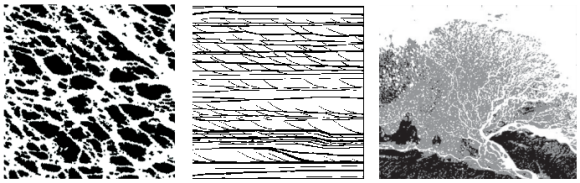


Figure 1: Examples of training images used in different applications. Left: Training image used for the modelling of interstitial cells of Cajal networks (Gao et al., 2015). Middle: Training image used for the modelling of small-scale sedimentary heterogeneities (Huysmans and Dassargues, 2009). Right: Example of a training image derived from a satellite image of the delta of a river (Hu et al., 2013).

Most of MPS algorithms differ from each other in the way that the training image is scanned and how the patterns extracted from it are stored and retrieved as the simulation proceeds. In general, MPS algorithms follow a sequential process; they simulate one, or a group of points at a time conditional to previously simulated points and hard data present on the simulation grid. As a starting point, the grid only contains hard data and then it is filled as the simulation progresses. At every uninformed grid node, the MPS algorithm extracts the existing data on the grid, both hard and previously simulated, given a search neighbourhood (or template) and then the method will try to find some matching patterns in the training image. A data template τ comprises n pixel locations $u_j = u_0 + h_j, j = 1,...,n$, defined by the n vectors $\{h_j, j = 1,...,n\}$ separating each location u_j from the template central node u_0. It is noteworthy that the selection of a particular template is an important decision as the template size directly affects the type of structures that can be modelled. A wise approach is to analyse the type of structures present in the training image and then to use a template of comparable size with what was observed (Mariethoz and Caers, 2015). Figure 2 presents an example with different templates in two dimensions.

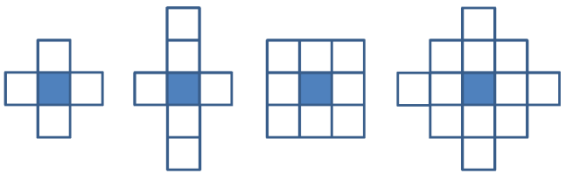


Figure 2.2: Different templates with 5, 7, 9 and 13 nodes. The central node is highlighted in blue.

Similarly, a data event for a given template τ consists of all the data available at informed locations within the template neighbourhood centred in the central node. The value at the central node of a template has to be determined such that it

shows spatial correlation with data values at the locations in the template. Most of simulation methods aim to compute the probability distribution function (pdf) for a central node x_0 of a data event. Figure 3 presents an example of a training image and the data events that it is comprised of.

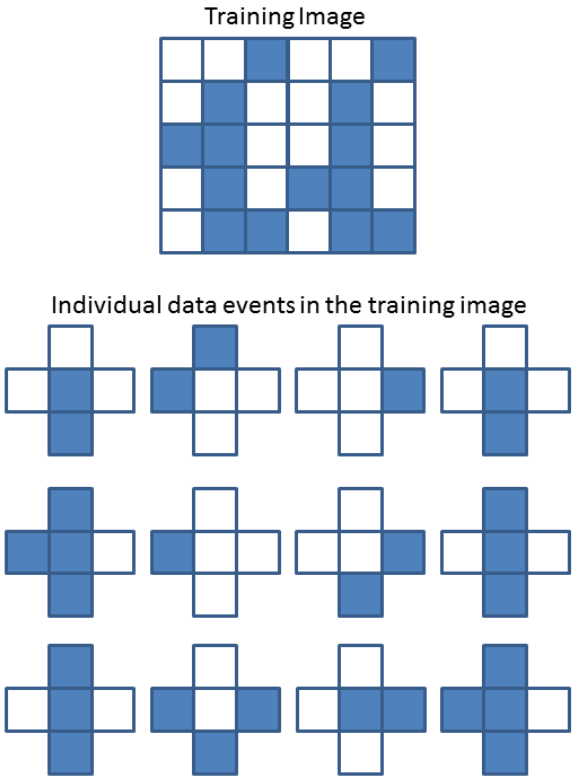


Figure 3: Example of a training image and all the data events present on it using a 5 nodes template (the left most template in Figure 2).

Sometimes it is necessary to model spatial patterns which are present at different scales, so a fixed template may fail to capture all of the variability present in the training image, for this reason the concept of multiple grids was introduced to overcome this obstacle. The idea is to include different scales by nesting several templates representing different scales, the original search template τ is correspondingly rescaled for each sub-set grid of the original simulation grid (Tran, 1994), this rescaling of the original template may be isotropic or anisotropic, depending if the expansion factor in each direction is the same or not (Remy et al.,2009).

The definition of a good match between a data event and the patterns in the training images differs for each algorithm and will depend if categorical or continuous variables are being analysed. Once matching patterns are found, the simulated values for the central node are chosen either by taking it from the best matching pattern or through a Monte Carlo simulation of the set of reasonably matching patterns (Boucher, 2013). The main idea is to search within the training image for the pattern most similar to any specific local conditioning data event existing in the numerical model being built. As a whole, MPS algorithms are a great communication tool between geoscientists and modellers since the geological concepts are passed as an image instead of a mathematical function. In this sense the training image is a bridge between the geological knowledge of the reservoir structures and patterns and the numerical model.

2.2 FILTERSIM - Filter Based Simulation

The previous sections introduced some of the basic concepts behind MPS simulation. The aim of this section is to present the FILTERSIM algorithm and some of the theoretical concepts on which it is based. The FILTERSIM algorithm was proposed by Zhang et al. (2006) and it was implemented in the SGeMS software by Wu et al. (2008). Most of this section is based on both works. In brief, FILTERSIM proceeds in three major steps: (1) filter score calculation, (2) pattern classification and (3) pattern simulation. The following subsections present a more detailed review of the entire simulation process.

2.2.1 Filter Score Calculation

The algorithm starts applying a set of filters to template data obtained from scanning the training image once per each template size. This search creates a set of filter score maps, with each training pattern represented by a low-dimensional vector of score values. A vector with these values describes local and directional mean levels, gradients and curvatures of the spatial pattern present in that template. This process significantly reduces the pattern data dimension from the template size to a small number of filter scores (default values implemented in SGeMS are 6 in 2D and 9 in 3D).

Formally, a filter is a set of weights associated with a specific template neighbourhood τ of size J, $\tau_J = \{u_0; h_j, j = 1,..., J\}$, where each node $u_j = u_0 + h_j$ of the template is characterized by a relative offset vector $h_j = (x_j, y_j, z_j)$ from the template central nodel u_0. Assuming that there are L filters for a size J template, the lth filter is $\{f_l(h_j); j = 1,..., J\}$ and that the training pattern pat centred at node u of a template τ_J is contained by the vector of L filter scores $\{S_\tau^l(u); l = 1,..., L\}$, with:

$$S_\tau^l(u) = \sum_{j=1}^{J} f_l(h_j) \cdot pat(u + h_j), \qquad (1)$$

where $pat(u + h_j)$ is the pattern nodal value. The corresponding filter score value is assigned to the central node u of the template and its value represents one particular aspect of the pattern considered. Accordingly, only one filter is not enough to capture all the variability in one particular pattern so a set of L filters is needed, with each filter highlighting a particular aspect of that pattern (Zhang et al., 2006).

2.2.2 Pattern Classification

Similar training patterns will have similar vector scores. Hence by partitioning the filter score space, similar patterns can be grouped together. Each pattern class may be represented by a pattern prototype, defined as the point-wise average of all training patterns falling into that class. A prototype has the same size as the filter template and is

used as the pattern group ID, a summary of all patterns falling into that class.

In the continuous case, a prototype *prot* associated with a search template τ_J is the point-wise average of all its constitutive replicates:

$$prot(h_j) = \frac{1}{c}\sum_{i=1}^{c} pat(u_i + h_j),\ j = 1,...,J, \qquad (2)$$

where h_j is the *j*th offset location in the search template τ_J, c is the number of replicates within that prototype class; $u_i (i = 1,...,c)$ is the center of a specific training pattern.

Two popular methods of classification are cross partition and K-mean clustering (Remy et al., 2009). The cross partition consists of partitioning independently each individual filter score into equal frequency bins while K-means clustering, given an input number of clusters, will find the optimal centroid of each cluster, and assign each training pattern to a specific cluster according to a distance between the training pattern and the cluster centroid. In the examples presented in this paper the first option was selected as this gave us faster results with similar outputs.

2.2.3 Stochastic Pattern Simulation

Based on the previous classification of the training patterns, sequential simulation can now be applied to build the simulated realizations. A sequential simulation approach is performed visiting each node of the current grid along a random path, different for each of the nested multiple grids used. At each node u along the random path visiting the simulation grid G, a search template τ of same size as the filter template is used to extract the conditioning data event $dev(u)$. The prototype *prot* closest to that data event is found based on a distance function $\delta(dev, prot)$. A pattern *pat* is drawn from that closest prototype class and pasted onto the simulation grid G. The inner part of the pasted pattern is frozen as hard data (also known as patch data), and will not be revisited during simulation on the current (multiple) grid.

The multiple grid simulation concept (Tran, 1994) is used to capture the large-scale structures of the training image with a large but coarse template τ. Denoted by G the three dimensional Cartesian grid on which simulation is to be performed, define G^g as the *g*th sub-set of G such that: $G^1 = G$ and G^g is obtained by down-sampling G^{g-1} by a factor of 2 along all three coordinate directions: G^g is the subset of G^{g-1} obtained by retaining every other node of G^{g-1}. G^g is called the *g*th level multi-grid.

In the *g*th multiple grid G^g, the search template τ_J is correspondingly rescaled by a factor 2^{g-1} such that:

$$\tau_J^g = \{2^{g-1}h_1,...,2^{g-1}h_J\} \qquad (3)$$

template τ_J^g has the same number of nodes as τ_J but has a greater spatial extent, hence allows capturing large-scale structures without increasing the template size. During the simulation in the *g*th coarse grid, the rescaled filters are used to calculate the pattern scores. Sequential simulation proceeds from the coarsest grid to the finest grid and all nodes simulated in the coarser grid are re-simulated in the next finer grid (Wu et al., 2008).

3. GEOSTATISTICAL MODELLING OF GEOTHERMAL RESERVOIRS

In an early paper from the authors (Vidal and Archer, 2015) a simple example of a stratified reservoir was presented. In that work the continuous value of permeability was considered as the uncertain value that is modelled through the system. In the examples presented in this work the aim is to try to reproduce a more complex geometry based on categorical information about rock types from a set of vertical wells from a real geothermal system. Figure 4 presents the spatial distribution of these wells and the different geological units that can be observed in each of them along with bar charts with the frequency of each unit. Additionally, in actual applications rock type data from surface outcrops should be included as hard-data if they are available. As can be seen from Figure 4 well data is mainly concentrated in the central part of the system with some wells in the north-west side and in the south-east part of the area of interest. Deep data is only available in the central and the south-east part where the deepest wells reached around 2,000 m below the surface. For confidentiality reasons the location and name of this geothermal system and the names of the wells and geological units are not mentioned, but the resulting geological model and geostatistical realizations are presented.

3.1 Construction of Training Images

The first step for the modelling of a reservoir using MPS algorithms is the construction of a proper TI that reflects geometric aspects of rock patterns considered to prevail in the actual reservoir. In the case of geothermal reservoirs, these are normally composed of geological units that do not show a repetitive pattern in space, which is a bit different from the original concept of a TI as a repository of repetitive patterns, as could be expected for some oil and gas reservoirs where MPS algorithms have been widely used. As was discussed by Boucher et al. (2014), this is also the case in the mining industry where the location of each geological unit is partially known from drilling, but it is their extent and geometry that is uncertain. In these applications it is normal to have access to some kind of three dimensional geological model based on well data and previous knowledge and in this case the aim of the simulation process is to perturb this original block model and generates an ensemble of realizations for uncertainty characterization.

For the construction of this first geological model (TI), the three dimensional geological modelling software Leapfrog Geothermal was used. This model was then exported into a regular grid composed of 37 x 57 x 21 blocks in the x, y and z directions, respectively with a block dimension of 100 x 100 x 100 m. It is a common practice in problems where the aim is to simulate repetitive patterns to use a TI which is defined in a larger grid than the simulation grid of interest,

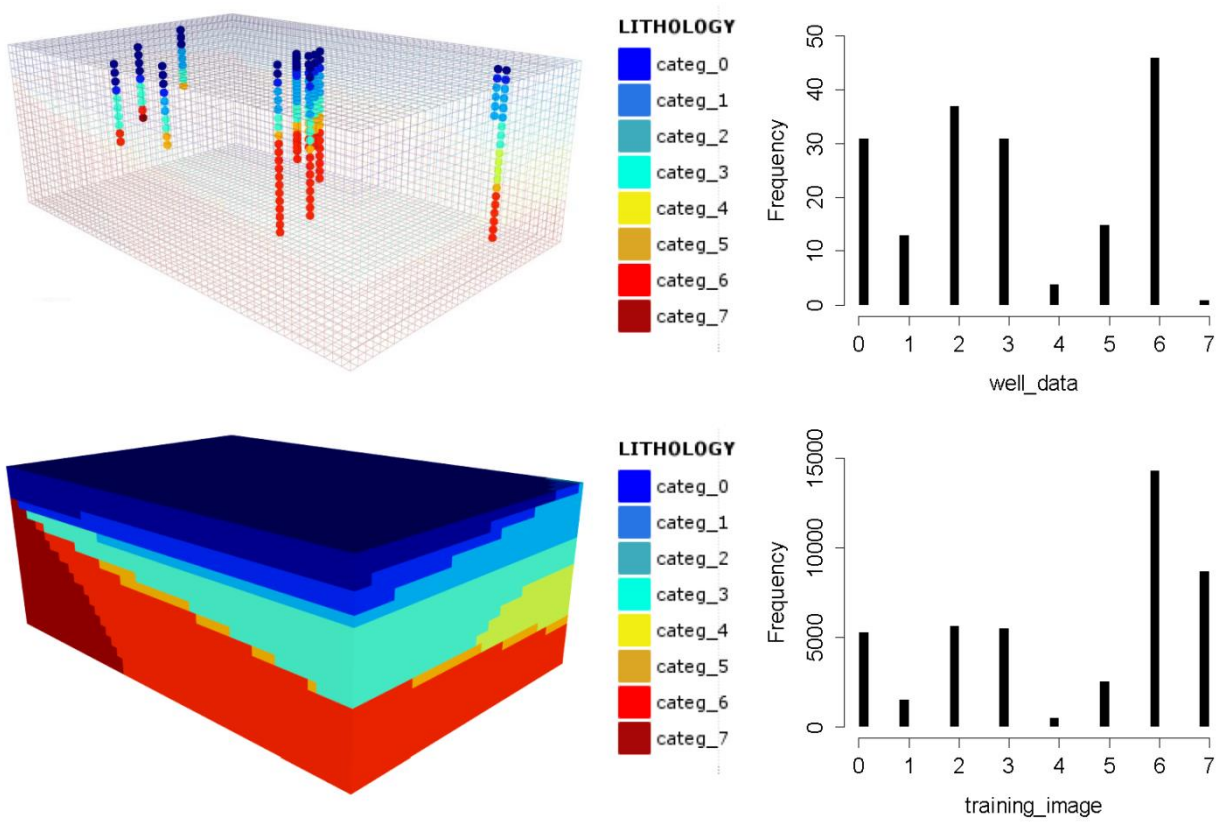


Figure 4: Upper figure: Location and rock type data observed in a set of wells. Lower figure: Geological model used as a TI. Additionally, bar charts showing the frequency of different categories for both sets of data are shown.

so more patterns may be recovered from the TI and stored by the algorithm, but in the case of a geothermal system we preferred to use a TI that is defined in the same simulation grid as has been done in some mining applications due to the non-repetitive character of the geological units present (Osterholt, 2007; Goodfellow et al., 2012). Figure 4 presents a geological interpretation of the reservoir under study, which will be used as a TI, and the resulting frequencies after translating this model into the simulation grid. The main difference which can be observed between both bar charts is the frequency of unit categ_7 as the TI holds a larger proportion than the observed in well data. This is due to the fact that unit categ_7 is only observed in one well, while the geological model takes into account the interpreted geometry of this unit. The resulting TI, includes most of the aspects considered to prevail in an actual geothermal reservoir hosted in a volcano-sedimentary basin, there are continuous geological units with a variable thickness, as could be expected for some tuffs, lavas or ignimbrites and local, spatially restricted units with curvilinear patterns, such as rhyolitic domes or high-viscosity lavas.

3.2 Results

With the TI and the simulation grid defined a set of FILTERSIM realizations were carried out using the software SGeMS (Remy et al., 2009). Figure 5 presents a small subset of these realizations after a manual calibration process for the FILTERSIM initial parameters with the aim to obtain realizations that show variability between them, and keeping the most important features of the original hard-data and TI. From this process of calibration it was clear that, in this particular case, the most influential parameters, conditioned on a single TI, are the size of the search template and the inner patch, less influential but still important are the number of multigrids, that in our models varies between 3 to 5 and the initial number of clusters for pattern classification purposes. Similarly, and as may be expected, the choice of a particular TI may have important consequences for the resulting realizations. Figure 6 presents some realizations produced with alternative TIs to those presented in Figure 5. For the purposes of geological uncertainty quantification and depending on the degree of knowledge about the current field, the use of more than one TI must be considered. For example, if the available geological model (TI) generates enough consensus between collaborators, then with only one TI and slight modifications to this model should be adequate, but in the case of significant uncertainties different TI that emphasize different, but equivalent, interpretations of the geological structure must be included. This is the case presented in Figure 6 where alternative TI imposes wider distributions for units categ_4 and categ_7 than in the previous examples, as these units are the less constrained by well data, so its spatial distribution is more uncertain. Moreover, TIs may add extra variability to the generated models, which is an important feature for spatial uncertainty quantification if it is thought that the available hard data from wells does not encompass the full variability of the phenomena it may be included with the selection of a proper TI.

Unlike the synthetic examples presented in Vidal and Archer (2015), where it was straightforward to conduct

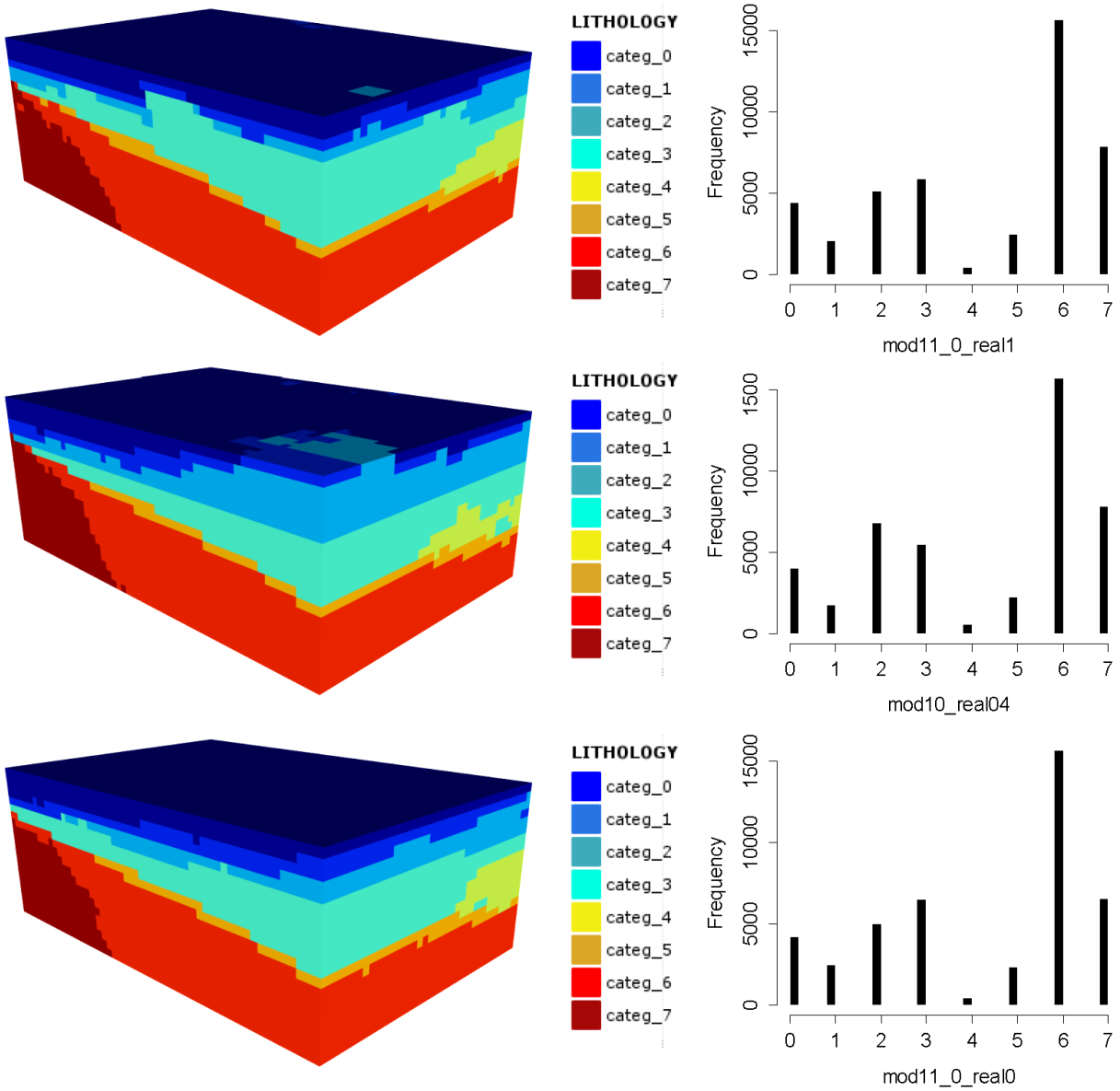


Figure 5: Three different FILTERSIM realizations of the geological structure of the reservoir under study using the TI presented in Figure 4. Additionally, bar charts showing the frequency of different categories for the different models are shown.

AUTOUGH2 flow evaluations using the generated geological realizations of the permeability field, in the current case only the geometries and extension of geological bodies were modelled and no information about the permeability values was considered. One simple approach could be to assign the most likely value of permeability for each geological unit from some previous knowledge of experts and then evaluate each realization in the flow simulator, or to populate each geological unit with permeability values from a particular prior distribution or variogram using, for example SGSIM realizations. The main difficulties with both approaches in a context of model calibration is that they need some form of previous knowledge about the values of permeability for each geological unit, which may not always be available, and that it is not efficient to evaluate each geostatistical realization in the flow simulator. In a paper in preparation by the same authors we will present an efficient optimization method that calibrates the permeability values of geological units to available measurements while varying the geological realizations as well. This approach is based on the use of surrogate modelling and considers the different geological models as a categorical input while the permeability values are treated as continuous variables.

4. CONCLUSIONS

Geothermal reservoir modelling, as well as other disciplines based on subsurface flow characterization, requires to include a quantification of geological uncertainty as flow behaviour is strongly dependent on the distribution of geological units. Reservoir simulation including geostatistical models helps to quantify and reduce the existing uncertainty based on available measurements (hard data) and in numerical representations of the expected spatial variability (variogram or TI) by means of a set of

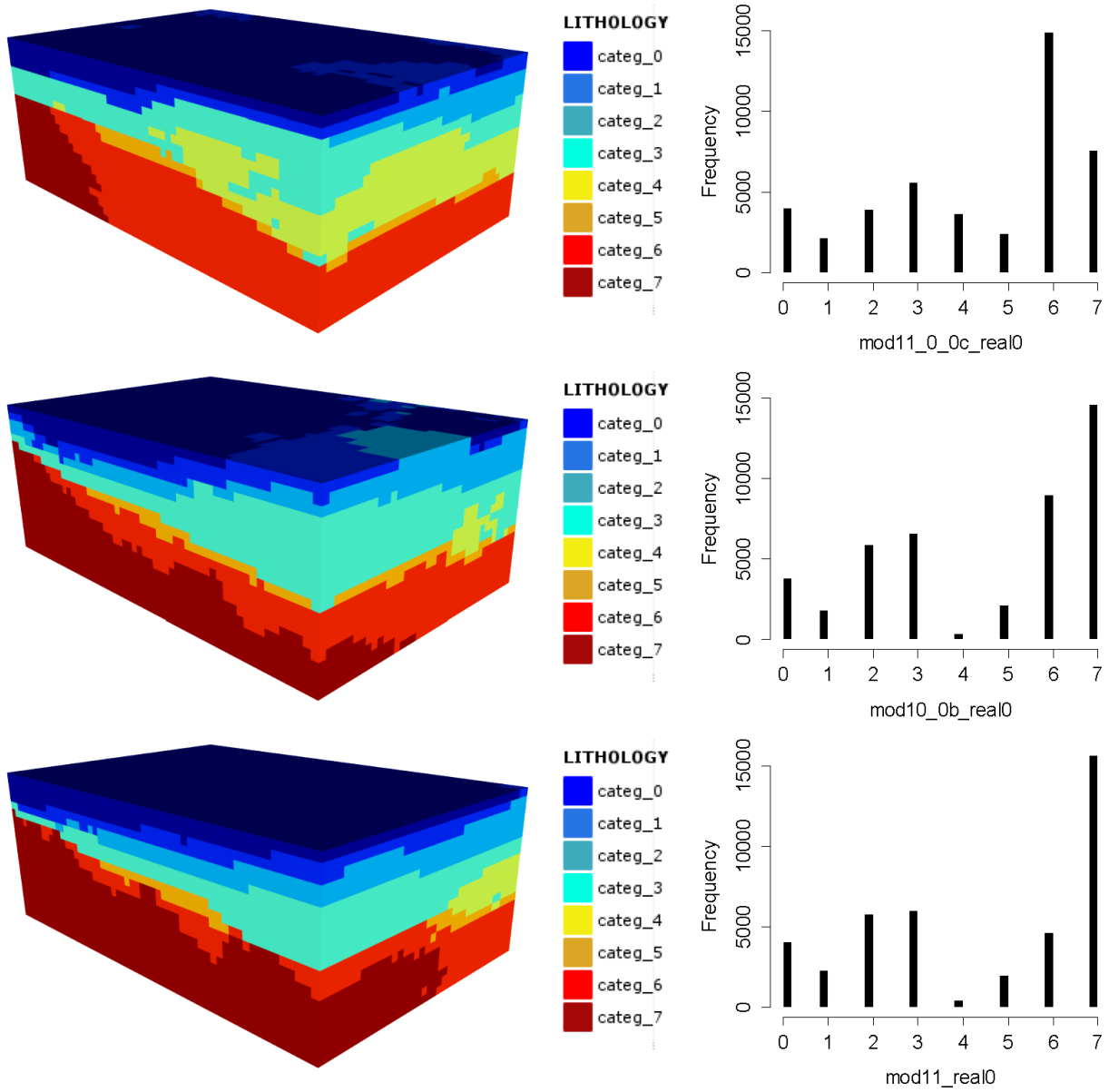


Figure 6: Three different FILTERSIM realizations of the geological structure of the reservoir under study. Upper model is based on a TI that increase the distribution of unit categ_4 and lower and middle models are based on a TI that increases the distribution of unit categ_7. Additionally, bar charts showing the frequency of different categories for the different models are shown.

alternative realizations of the variable under study (rock type, permeability, porosity, etc.). Two-point-based models offer an easy and reliable method for interpolation and simulation. One important limitation with this technique arises from data confidence, as much of the inferences and posterior analysis depends on the number and the spatial distribution of hard data. Additionally, variability in two-point realizations seems to be constrained by variability observed in the hard-data, which may present some limitations if the number of data is not significant. In this sense, interpretations on peripheral zones must be taken carefully. For its part, MPS models represent a novel approach that does not rely on variogram models based on available hard data, but instead on a numerical representation of patterns/units deemed to prevail in the actual reservoir. This numerical representation, or TI, also presents the advantage that is easy to understand by others (non-modeller specialists) as the spatial variability is expressed as an image instead of a mathematical function like the variogram. A proper TI needs to incorporate all the previous knowledge available for the system under study that may affect flow behaviour and more than one TI, considering alternative scenarios, should be considered if a significant uncertainty about geological interpretations remains. Numerical flow models based on geostatistical realizations represent a powerful technique to constrain numerical models with geological knowledge and then, through a stochastic process or either by using an

optimization method, select the right set of input parameters that reproduce some measurements of interest.

REFERENCES

Boucher, A.: Strategies for modeling with multiple-point simulation algorithms. In: Garner D, Thenin D, Deutsch CV (eds). Closing the gap: advances in applied geomodeling for hydrocarbon reservoirs. (2013).

Boucher, A., Costa, J., Rasera, L., and Motta, E.: Simulation of geological contacts from interpreted geological model using multiple-point statistics. *Mathematical Geosciences*, 46(5):561-572. (2014).

Deutsch, C. V. and Journel, A.: GSLIB: geostatistical software library and user's guide. Oxford University Press. (1998).

Gao, J., Sathar, S., Ogrady, G., Archer, R., and Cheng, L. K.: A stochastic algorithm for generating realistic virtual interstitial cell of cajal networks. *Biomedical Engineering*, IEEE Transactions on, 62(8):2070-2078. (2015).

Goodfellow, R., Albor Consuegra, F., Dimitrakopoulos, R., and Lloyd, T.: Quantifying multi-element and volumetric uncertainty, Coleman McCreedy deposit, Ontario, Canada. Computers & Geosciences, 42:71-78. (2012).

Goovaerts, P.: Geostatistics for Natural Resources Characterization. Oxford University Press, New York. (1997).

Honarkhah, M. and Caers, J.: Stochastic simulation of patterns using distance-based pattern modeling. *Mathematical Geosciences*, 42(5):487-517. (2010).

Hu, L. Y., Liu, Y., Scheepens, C., Shultz, A. W., and Thompson, R. D.: Multiple-point simulation with an existing reservoir model as training image. *Mathematical Geosciences*, 46(2):227-40. (2013).

Huysmans, M. and Dassargues, A.: Application of multiple-point geostatistics on modelling groundwater flow and transport in a cross-bedded aquifer (Belgium). *Hydrogeology Journal*, 17(8): 1901-1911. (2009).

Journel, A. G.: Geostatistics for conditional simulation of ore bodies. Economic Geology and the Bulletin of the Society of Economic Geologists, 69(5): 673-687. (1974).

Journel, A. G.: Geostatistics: Roadblocks and Challenges, pages 213-224. Springer Netherlands, Dordrecht. (1993).

Mariethoz, G. and Caers, J.: Multiple-point geostatistics : stochastic modeling with training images. Wiley Blackwell. (2015).

Mariethoz, G., Renard, P., and Straubhaar, J.: The direct sampling method to perform multiple-point geostatistical simulations. *Water Resources Research*, 46(11). (2010).

Matheron, G.: Intrinsic random functions and their applications. *Advances in Applied Probability*, 5(3): 439-468. (1973).

Osterholt, V., D. R.: Simulation of wireframes and geometric features with multiple-point techniques: application at Yandi iron ore deposit. In: Orebody modelling and strategic mine planning, AusIMM, Spectrum Series, 2nd ed., 14:95-124. (2007).

Remy, N., Boucher, A., and Wu, J.: Applied Geostatistics with SGeMS - A User's Guide. Cambridge University Press. (2009).

Straubhaar, J., Renard, P., Mariethoz, G., Froidevaux, R., and Besson, O.: An improved parallel multiple- point algorithm using a list approach. *Mathematical Geosciences*, 43(3):305-328. (2011).

Strebelle, S.: Conditional simulation of complex geological structures using multiple-point statistics. *Mathematical Geology*, 34(1):1-21. (2002).

Tran, T. T.: Improving variogram reproduction on dense simulation grids. *Computers & Geosciences*, 20(7-8):1161-1168. (1994).

Vidal, A. and Archer, R.: Geostatistical simulations of geothermal reservoirs: two-and multiple-point statistic models. *Proc. World Geothermal Congress 2015*. Melbourne, Australia. (2015).

Wu, J., Boucher, A., and Zhang, T.: A SGeMS code for pattern simulation of continuous and categorical variables: FILTERSIM. *Computers & Geosciences*, 34(12):1863-1876. (2008).

Zhang, T., Switzer, P., and Journel, A.: Filter-based classification of training image patterns for spatial simulation. *Mathematical Geology*, 38(1):63-80. (2006).